Supporting Information

Photoresponsive Cu-Covalent Organic Polymer as Multifunctional Artificial Enzymes for Synergistic Infected Wound Therapy

Chunzhen Zhao,[a,d#] Changxiao Du,[c,d#] Jie Xu, [a#] Yuqing Zhao,[d#] Xiaoming Shi,[e] Dong Zhang,[e] Xinmiao Zhang,[d] Yi Zhang,[d] Han Sun,[d] Xixin Jiang,[d] Zhen Du,[d] Mengjin Wang,[d] Meimei Xiao,[c*] Mingwen Zang[b,c*]

a. *Affiliated Hospital of Shandong Second Medical University, Shandong Second Medical University, 261053 Shandong, PR China.*

b. *Weifang Brain Hospital, Weifang, Shandong, PR China*

c. *Weifang People's Hospital, Shandong Second Medical University, Weifang, Shandong, PR China.*

d. *School of Pharmacy, Shandong Second Medical University, Weifang, 261053 Shandong, PR China*

e. *Shandong Neptunus Galaxy Pharmaceutical Co., Ltd, Weifang, Shandong, PR China.*

[#] These authors contribute equal to this work.

* *Corresponding author.* Meimei Xiao, Mingwen Zang

E-mail: 511017186@qq.com (M. Xiao); 806002570@qq.com (M. Zang)

Contents

Section 1. Materials

Section 2. Methods

Section 3. ^{1}H-NMR

Section 4. N_2 adsorption isotherm of PEB-COP-Cu.

Section 5. Pore size distribution curve of PEB-COP-Cu.

Section 6. EDS spectra of PEB-COP-Cu.

Section 7. UV-visible spectra and working curve of PEB-COP-Cu.

Section 8. Light and water stability of PEB-COP-Cu.

Section 9. Effect of temperature on the POD and OXD enzyme activities of PEG-COP-Cu.

Section 10. Photothermal antibacterial effects of PEB-COP-Cu at different concentrations.

Section 11. Biocompatibility testing of PEB-COP-Cu.

Section 12. Blood tests in PEB-COP-Cu treated mice.

Section 13. Supporting Tables

Section 14. Supporting References

Section 1. Experimental Section

1.1. Materials

All raw materials and reagents used to synthesize the complexes were provided by commercial suppliers and were not further purified unless otherwise stated. DMF was purified to dry DMF by redistillation with CaH2.Pyrrole was temporarily redistilled before use.

1.2. Synthesis of 1,3,5-tris(3-dimethylamino-1-oxoprop-2-en-yl)benzene (TDOEB)[1]

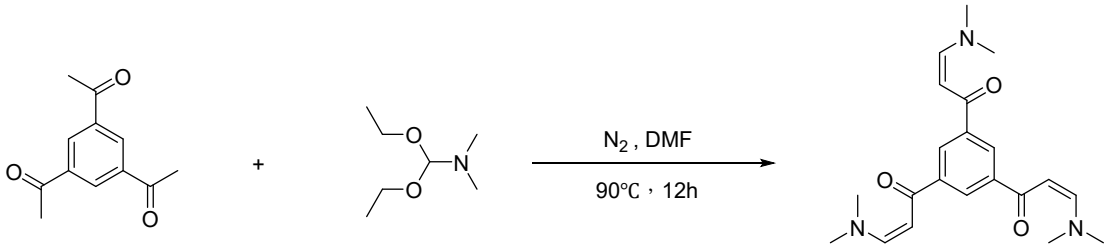

In a 100 mL flask, 1, 3, 5-triacetylbenzene (1.23 g, 4.0 mmol) and *N, N*-dimethylformamide diethyl acetal (3.6 g, 12.0 mmol) were added, following by the injection of 25 mL DMF. The mixture was sonicated for 2 min, which was then stirred for 12 h at 90 °C under the protection of N_2. The products were obtained by addition of Et_2O as yellow microcrystals in high yields. The crystals were washed with pentane (50.0 mL x 3), which was then dried in vacuum (Yield: 95%). ^{1}H NMR (400 MHz, Chloroform-d): δ 8.52 (s, 3H), 7.82 (d, J = 12.2 Hz, 3H), 5.85 (d, J = 12.3 Hz, 3H), 3.04 (d, J = 85.5 Hz, 18H).

1.3. Synthesis of 5, 10, 15, 20-Tetrakis(4-aminophenyl)porphyrin (TAPP)

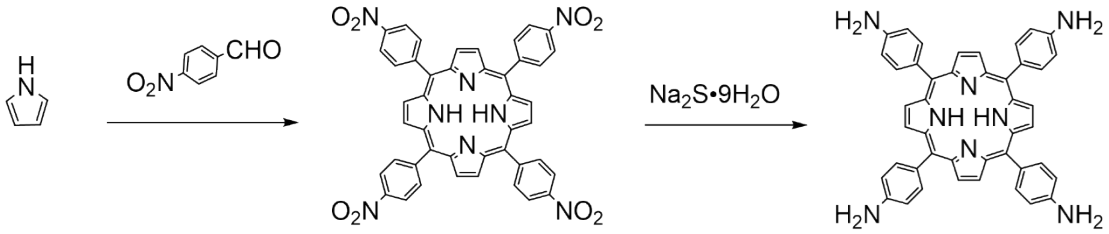

TAPP was synthesized with reference to previous literature. P-nitro benzaldehyde (11.3 g, 75 mmol), acetic anhydride (14 mL, 151 mmol) and propionic acid (200mL) were mixed in a 500 mL flask. The reaction system was heated to 140 °C. Subsequently, freshly distilled pyrrole (5.2 mL, 75 mmol) was injected into the reaction system dropwise, which was refluxed for 30 min. Then, the heating was stopped, and the reaction mixture was cooled down to room temperature. Afterwards, the precipitate was obtained by filtration, which was washed with DMF and hot water until it was colorless.

The product was dried in a vacuum drying oven to obtain 5, 10, 15, 20-tetrakis(4-nitrophenyl)porphyrin (TNPP, 1.21 g, yield: 24%).

TNPP (0.10 g, 25 mmol), Na2S·9H2O (0.604 g, 2.5mmol) and NH4Cl (0.06g, 0.1 mmol) were added to a 100 mL three-neck flask. Then, under the protection of argon, DMF (6 mL) and distilled water (0.2 mL) was injected. Subsequently, under stirring, the reaction system was heated to 90 °C, which was maintained for 3 h. Afterwards, the reaction system was cooled down to 80 °C, followed by the addition of 20 mL of distilled water dropwise. After cooling down to the room temperature, the precipitate was filtrated, which was washed with water until the filtrate was colorless and neutral. The final product was dark purple solid obtained by room temperature vacuum drying (0.079 g, yield: 94%).

1.4. Synthesis of PEB-COP

The synthesis of PEB-COP was referenced in the previous literature. To a 10 ml plastic centrifuge tube, TDOEB (18.5 mg, 0.05 mmol) and TAPP (33.7mg, 0.05 mmol) were suspended in 4.0 ml of aqueous solution, then 0.4 ml of acetic acid was added as catalysts. The mixture was kept at room temperature and ambient pressure for 8 h. The precipitate was then filtered, washed subsequently with DMF (3 x 10.0 mL), acetone (3×10.0 mL), and hexane (3×10.0 mL), which was then dried under vacuum at 100 °C overnight to give an orange solid (87% yield).

1.5. Synthesis of PEB-COP-Cu

Synthesis of PEB-COP-Cu. 1 mg of PEB-COP was immersed in 50 mL of 5.0x10-2 mol/L copper acetate solution and stirred at 80 °C for 24 h. The solution was filtered and washed several times with deionized water to remove excess metal ions to obtain PEB-COP-Cu.

1.6. Synthesis of PEB-COP-Cu

2. Methods

2.1. Material characterization

The ^{1}H-NMR spectra of the prepared monomers were recorded by Avance Bruker DPX 400 (400 MHz). Fourier transform infrared spectroscopy (FT-IR, PerkinElmer, 2000 FTIR spectrometer, Cambridge, UK) was recorded at wavelengths ranging from

400 to 4000 cm^{-1}. Solid-state ^{13}C CP/MAS NMR were collected on Bruker SB Avance III 500 MHz spectrometer. The morphology of the powder samples was evaluated with a field emission scanning electron microscope (SEM, Ultra 55) and a transmission electron microscope (TEM, Tecnai G2 20 TWIN) by immersing the prepared samples on a copper grid. N_2 adsorption and desorption measurements were carried out on a Belsorp max analyzer (Japan) at a low temperature of 77 K. Thermogravimetric analysis (TGA) was recorded with a microcomputer differential heat balance analyzer (HCT-1, Hengjiu Corporation, Beijing, China) under nitrogen protection. The UV-visible spectra were obtained by Shimatsu UV 2600 spectrophotometer (Shimadzu, Japan) in the range of 200 nm to 800 nm. Powder X-ray diffraction (XRD) parameters were obtained in the range of 5°to 80°using a Rigaku SmartLab, Japan, Cu target, wavelength 1.5406Å; operating voltage 40KV; operating current 150mA. X-ray photoelectron spectroscopy (XPS) testing using ThermoFischer ESCALAB 250Xi. EPR test through the instrument Bruker A300. Frequency: 9.853GHz; Power: 10.8mW; Center field: 3510G; Scanning width: 100G; Modal amplitude: 1G; Time constant: 1.250mS; Scanning time: 19.456S. XPS reflects the elemental composition of the surface within 1–10 nm and EDS reflects the average content of the bulk phase within hundreds of nanometres.

2.2. Photothermal performance

Temperature changes during irradiation were monitored using an infrared thermographic camera, and images of temperature changes at different time points were recorded.

Effect of different concentrations: 1 mL of aqueous suspension of PEB-COP-Cu at concentrations of 0, 50, 100, 150, 200, and 250 μg/mL was added to a 2 mL EP tube and then irradiated with a 638 nm laser at a power density of 1.5 W/cm^2 for 10 min. Effect of varying power: PEB-COP-Cu at a concentration of 250 μg/mL was irradiated with a 638 nm laser at power densities of 0, 0.5, 0.75, 1, 1.2, and 1.5 W/cm^2 for 10 min.

Cu^{2+} effect: PEB-POP and PEB-COP-Cu at 250 μg/mL were irradiated with a 638 nm laser at a power density of 1.5 W/cm^2 for 10 min.

Photothermal stability: The photothermal stability of PEB-COP-Cu was evaluated

by ON/OFF cyclic irradiation. The 638 nm laser was used to irradiate 1 mL of a 250 μg/ml aqueous suspension of PEB-COP-Cu for 10 min, then the laser was turned off and the PEB-COP-Cu was allowed to cool naturally to its starting temperature. Five laser cycles were repeated in the same manner. Temperature changes were recorded throughout the experiment.

Calculation of photothermal conversion efficiency: The aqueous dispersion of PEB-COP-Bu was irradiated with a laser (λ = 638 nm, 1.5 W/cm2) for 10 minutes. Then, natural cooling was waited for and the heating and cooling processes were monitored in real time using a thermometer with a thermocouple probe. The photothermal conversion efficiency (η) is calculated by the following equation：

$$\eta\ (\%) = [hS\ (T_{max}–T_{surr})–Q_{dis}]/I(1–10^{–A\ 638}) \quad (S1)$$

The meaning of each element in the formula is given as follows: 'h' is the heat transfer coefficient; 'S' is the surface area of the vessel; 'T_{max}' is the equilibrium temperature after 10 minutes of irradiation (53.7°C); 'T_{surr}' is the ambient temperature at the time of the experiment (26.5°C); 'Q_{dis}' is the heat dissipation of the test cell (25.03 mW); 'I' represents the laser power at 638 nm (1.5 W/cm^2). 'A638' is the absorbance of PEB-COP-Bu aqueous solution at 638 nm (0.4894).

$$hS = m_{H2O}\, C_{H2O} /\tau_S \quad (S2)$$

$$t= -\tau_S\, (In\theta) \quad (S3)$$

The meanings of each element in the formula are also listed: 'm_{H2O}' is the mass of water solvent (1×10^{-3} kg) at the time of experiment; 'C_{H2O}' is the specific heat capacity of water (4.2×10^3 J/kg °C); τ_S is the PEB-COP-Bu time constant (250); 'θ' is the ratio of ΔT and T_{Max}. So, in this experiment, $\eta\ (\%) = [hS\ (T_{max} – T_{surr}) – Q_{dis}] / I\ (1 – 10^{-A\ 638}) = 42.6\%$.

2.3. OXD-like activity of PEB-COP-Cu

Briefly, 50 μL of PEB-COP-Cu (1.0 mg-mL-1) and 50 μL of TMB (5.0 mM) were mixed in 100 μL of PBS buffer (0.01 M, pH 3.5), and then reacted at 35 °C for 30 min. Absorbance values at 652 nm were recorded using UV-visible absorption spectroscopy. Subsequently, the effect of pH on absorbance was tested in PBS at different pH. To investigate the effect of O_2 on the oxidation of TMB, PBS buffer solution (0.01 M, pH 3.5) was bubbled with O_2 and AR2and air for 30 min prior to the

test, and other test conditions were kept constant. The effect of different free radical scavengers on the activity of PEB-COP-Cu-like OXDs was investigated. At the beginning of the experiment, 50 μL of PEB-COP-Cu (1.0 mg-mL-1) and 50 μL of TMB (5.0 mM) were mixed in 850 μL of PBS buffer (0.01 M, pH 3.5). Then, 50 μL of free radical scavengers, i.e., IPA, HD, BQ, and EDTA at a concentration of 5.0 mM, were added. the reaction mixture was incubated at 35 °C for 30 min, and then the UV-Vis absorption spectra of the reaction system were recorded.

2.4. POD-like activity of PEB-COP-Cu

50 μL of PEB-COP-Cu (1.0 mg-mL-1), 50 μL of TMB (5.0 mM), and 50 μL of H_2O_2 (10.0 mM) were mixed with 850 μL of PBS buffer (0.01 M, pH 3.5), and the reaction was carried out at 35 °C for 30 min, and then recorded with a UV-Vis spectrophotometer. In addition, the POD-like activity was evaluated by the same method in the presence or absence of laser, in PBS system solutions of different pH and at different PEB-COP-Cu concentrations, and the mechanism of PEB-COP-Cu POD activity was investigated in the same way as that of OXD activity.

2.5. Photodynamic testing of PEB-POP-Cu

Singlet oxygen ($^1O_2$) detection： 1,3-Diphenylisobenzofuran (DPBF) was used as a $^1O_2$-specific trapping agent for the measurement of the single-linear state of oxygen produced by PEB-COP-Cu. Specifically, a 1 mg/ml solution of DPBF DMSO was configured and the absorbance of DPBF at 421 nm was adjusted using a UV-visible spectrophotometer (Abs of about 1, concentration of about 10 μg/ml). PEB-COP-Cu (250 μg/ml) was then added to this cuvette and the change in absorbance of DPBF at a specific time under 1.5 W/cm^2 laser radiation was recorded. The ability of single-linear oxygen generation at different PEB-COP-Cu concentrations and at different laser powers was probed by the same approach.

Superoxide anion detection ($O_2^{\bullet-}$): Dihydrorhodamine (DHR) was used as a fluorescent probe for the generation of superoxide anion during the measurement procedure.1 μl of DHR,750 μl of PEB-COP-Cu (1 mg/ml) was added to 3 ml cuvette, diluted to 3 ml by adding PBS, and superoxide anion was generated during the measurement procedure under a 1.5 W/cm^2 laser.

2.6. In vitro antimicrobial performance testing

Individual colonies of Escherichia coli and Staphylococcus aureus, which were used as Gram-negative and Gram-positive bacterial models, respectively, were transferred to 5 mL of Luria-Bertani (LB) medium (containing trypsin 10 g/L, yeast extract 5 g/L, and sodium chloride 10 g/L, pH=7.4) and incubated in an incubator for 12 hours at 110 rpm at 37°C. The incubation was carried out at 37°C for 12 hours at 110 rpm in an incubator. Fresh strains in LB medium were diluted with phosphate buffered saline (PBS, pH=7.3) to obtain the desired concentration (OD600=0.1, equivalent to 1 × 108 CFU/mL).

Dispersions of different concentrations of PEB-COP-Cu were incubated with Staphylococcus aureus and Escherichia coli (100 μL, 1 × 108 CFU/mL) for 12 h at 37°C under light (λ = 638 nm, 1.5 W/cm^2, 10 min) or no light conditions. After gradient dilution, 80 μL of bacteria were transferred to solid medium, and the antimicrobial activity of PEB-COP-Cu was estimated by plate counting method, and all experiments were repeated three times. The antimicrobial properties under different grouped treatment conditions were tested according to the same method described above.

2.7. Live/dead staining of bacteria

To the above dispersions containing 100 μL of E. coli or Staphylococcus aureus (1 × 108 CFU) in different treatment groups, SYTO-9 and PI were added to differentiate between live and dead microbial cells after incubation with or without laser irradiation. Methods: 20 μL SYTO-9 (1. 0×10-3 M) and 20 μL PI (1.5×10-3 M), 37 °C, dark for 15 min. After staining, the samples were centrifuged in PBS to remove excess SYTO-9 and PI. the bacteria were then resuspended in 50 μL of PBS and placed on the surface of a slide. Images of E. coli or S. aureus are then captured using a fluorescent inverted microscope.

2.8. Transmission electron microscopy (TEM) of bacteria

Incubated solutions containing S. aureus or E. coli after the different treatments described above were taken. Bacteria were fixed in 2.5% glutaraldehyde solution (4°C, 24 h), rinsed three times with PBS, embedded in agar and blocked. Bacteria were then dehydrated by continuous treatment with ethanol solutions (30%, 50%, 70%, 90%, 95% and 100%) for 10 min at room temperature, then treated with acetone for 3 h at room

temperature, embedded in a gradient of embedding medium, negatively stained and sectioned on a nickel mesh. The nickel mesh was placed under TEM observation. The morphology was captured.

2.9. MTT experiment

In 96-well plates, 3T3 cells were inoculated at a density of 5 × 103 cells per well, with 180 μL of cells per well, and liquid-sealed by adding 200 μL of PBS to surrounding duplicate wells to prevent excessive cell evaporation. After 24 hours of incubation, 20 μL of the expanded tenfold concentration was added according to the grouping and concentration gradient of the in vitro antimicrobial assay, and the cells were incubated together for 72 hours in the presence of laser irradiation ((λ = 638 nm, 1 .5W/cm2, 10 min). 20 uL of MTT (5 mg/mL) solution was added to each well and incubation was continued for 4 h. The supernatant was discarded and 150 μL of DMSO was added and dissolved on a shaker for 10 min before the absorbance of the 96-well plate was measured by an enzyme meter at 570 nm. Each set of experiments was repeated three times.

2.10. Hemolysis testing

Fresh blood was obtained from KM female mice (Swiss mouse origin). Erythrocytes were collected by centrifugation at 15,000 rpm for 20 minutes and washed three times with PBS. The erythrocytes (4% w/w) were then incubated with PEB-COP-Cu at a ratio of 1:9 (v/v) for 3 hours at 37°C and then centrifuged at 12,000 rpm for 20 minutes. Then, 100 μL of supernatant from each group was placed in a 96-well plate and the absorbance of each group was measured at 570 nm using an enzyme meter. Distilled water was used as positive control and PBS as negative control. The amount of hemolysis was calculated by the following formula:

$$\text{Hemolysis (\%)} = (A\text{-}An)/(Ap\text{-}An) \times 100\% \quad (S4)$$

Where “A” is the absorbance obtained from the supernatant taken after addition of PEB-COP-Cu to the erythrocytes.Ap” is the absorbance of the supernatant taken after addition of distilled water to the erythrocytes (positive control).

2.11. Cell Scratching Experiment

The effect of PEB-COP-Cu on the migration of 3T3 cells was studied and

evaluated by performing a cell scratch assay. 3T3 cells were inoculated into 6-well plates and cultured to 90% density. The center of the 3T3 cell monolayer was gently and slowly scraped with a 20 μL pipette tip to form a cross in each well. Wash with PBS to remove detached cells, and then add fresh basal medium containing 250 μg/mL PEB-COP-Cu and basal medium without PEB-COP-Bu, respectively. Finally, micrographs of 3T3 cells in each well were taken at the indicated times.

2.12. Bacterial biofilm inhibition test

Staphylococcus aureus and Escherichia coli were used for modelling. 150 μL of liquid medium and 50 μL of bacterial solution were added to each well of a 96-well plate and incubated in an incubator for 72 h. The experiment was divided into control groups, *i. e.*, PBS group (I), PEB-COP group (II), PEB-COP-Cu group (III), PEB-COP-Cu+Laser group (IV), and PEB-COP-Cu+Laser+H_2O_2 group (V). In each of the above groups, 50 μL of PBS or PEB-COP dispersion solution or PEB-COP-Cu dispersion solution was added: 10uL of H_2O_2 was added to the H_2O_2 group; and the laser group was irradiated with a 638 nm, 1.5W/cm^2 laser for 10 min. Add the above groups into the cultured bacterial solution and incubate for 5 h. After incubation, stain with crystal violet (CV), rinse with PBS, fix with 100 μL methanol for 30 min, then rinse with PBS, finally add 0.1% crystal violet 50 μL and incubate for 20 min, after incubation, rinse with PBS until clarified, add glacial acetic acid 100 μL, then incubate for 30 min, aspirate the supernatant into a blank plate and measure the OD value (490 nm).

2.13. In vivo wound healing experiment

Wound healing was modeled using 5-week-old female KM mice (from Swiss mice) (5 mice per group, 20-25 g) divided into 6 groups. After disinfection with ethanol solution (75%), the dorsal hair of each mouse was shaved prior to surgery to form a d = 5 mm wound, which was then infected with Staphylococcus aureus (1 × 106 CFU/mL) for 24 hours. The wounds were then treated with PBS (I), PEB-COP-Cu (II), Laser (III), PEB-COP-Cu+H2O2 (IV), PEB-COP-Cu+Laser (V), and PEB-COP-Cu+H_2O_2+Laser (VI) (λ = 638 nm, 1.5W/cm^2 for 10 min, CPEB -COP-Cu/PEB-COP = 250 μg/mL) conditions were used to treat the infected wounds and photographs of the wound surfaces were taken on days 1, 3, 5, 7, 9, and 11 while monitoring the body

weight of the mice. Changes in wound size were measured using an image analysis program (Image. J, National Institutes of Health). All mice died on day 11. Wound skin tissue and major organs, including the heart, liver, spleen, lungs, and kidneys, were excised and fixed with 10% paraformaldehyde, followed by H&E staining and Masson trichrome staining. On day 11, 1 to 2 mL of blood samples were collected from the bottom of mouse arteries. 500 μL of each blood sample was taken for routine blood analysis, including leukocytes, erythrocytes, hematocrit, hematocrit, hematocrit, and hematocrit.

Section 3. ^{1}H-NMR

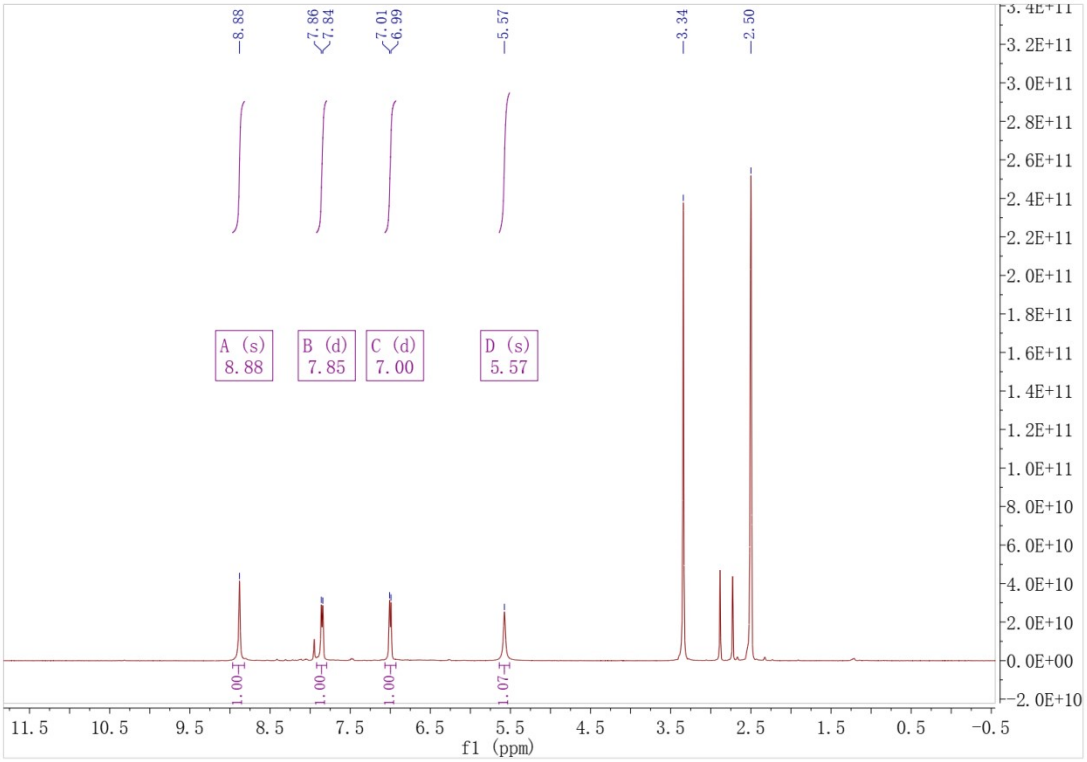

Scheme S1 ^{1}H-NMR of 5, 10, 15, 20-Tetrakis(4-aminophenyl)porphyrin (TAPP)

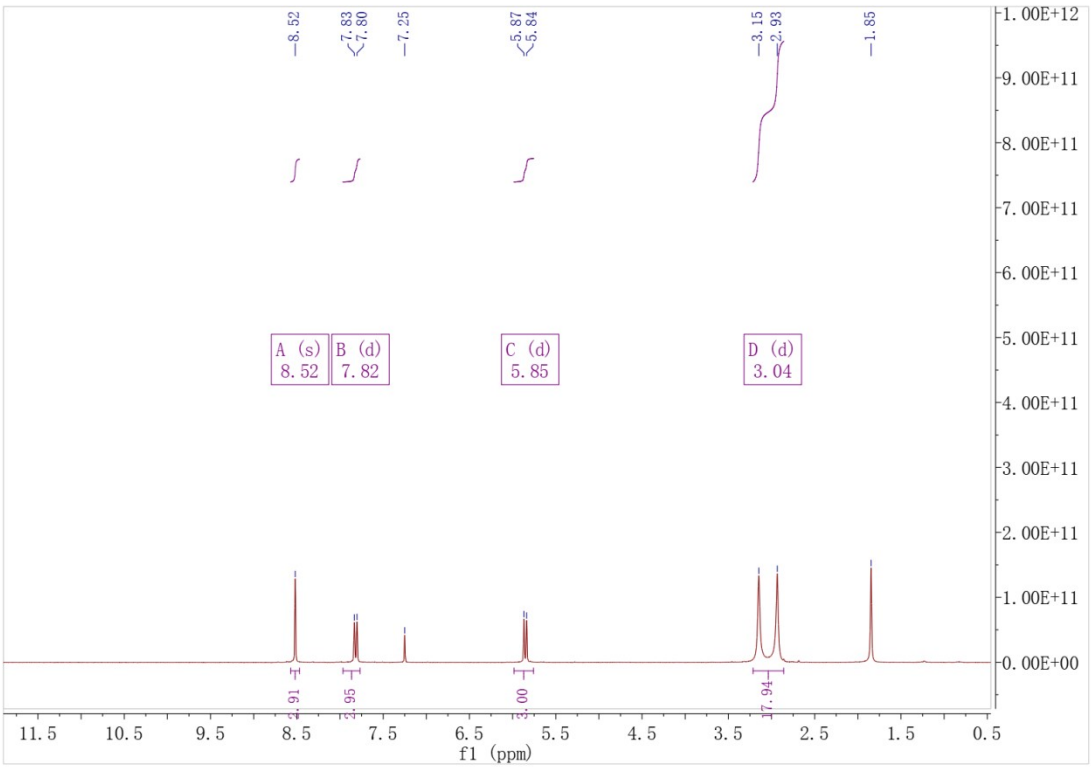

Scheme S2 ^{1}H-NMR of 1,3,5-tris(3-dimethylamino-1-oxoprop-2-en-yl)benzene (TDOEB).

Section 4. N_2 adsorption isotherm of PEB-COP-Cu.

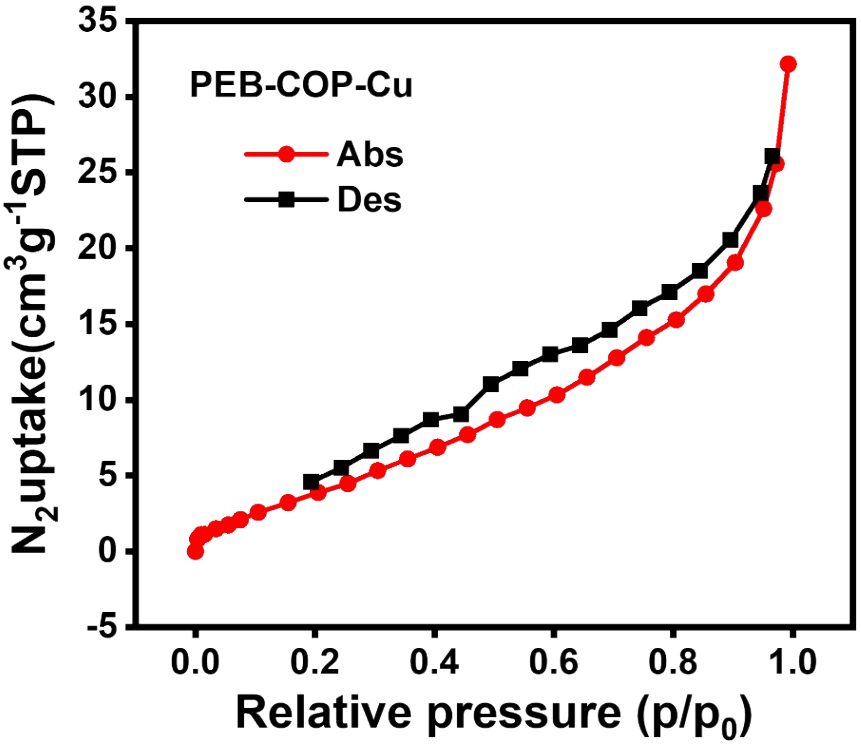

Fig. S1 The low-temperature N_2 adsorption isotherm of PEB-COP-Cu.

Section 5. Pore size distribution curve of PEB-COP-Cu.

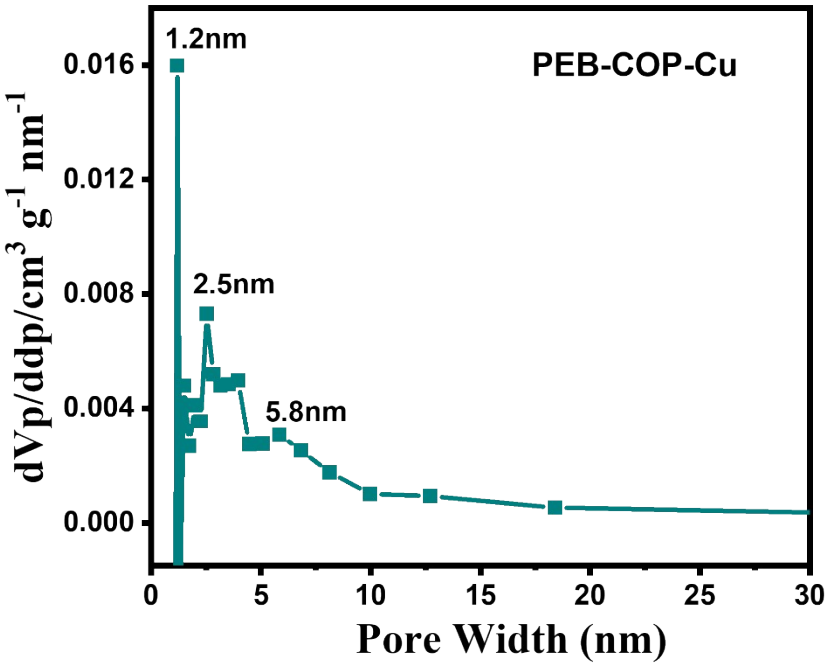

Fig. S2 Pore size distribution curve of PEB-COP-Cu.

Section 6. EDS of PEB-COP-Cu.

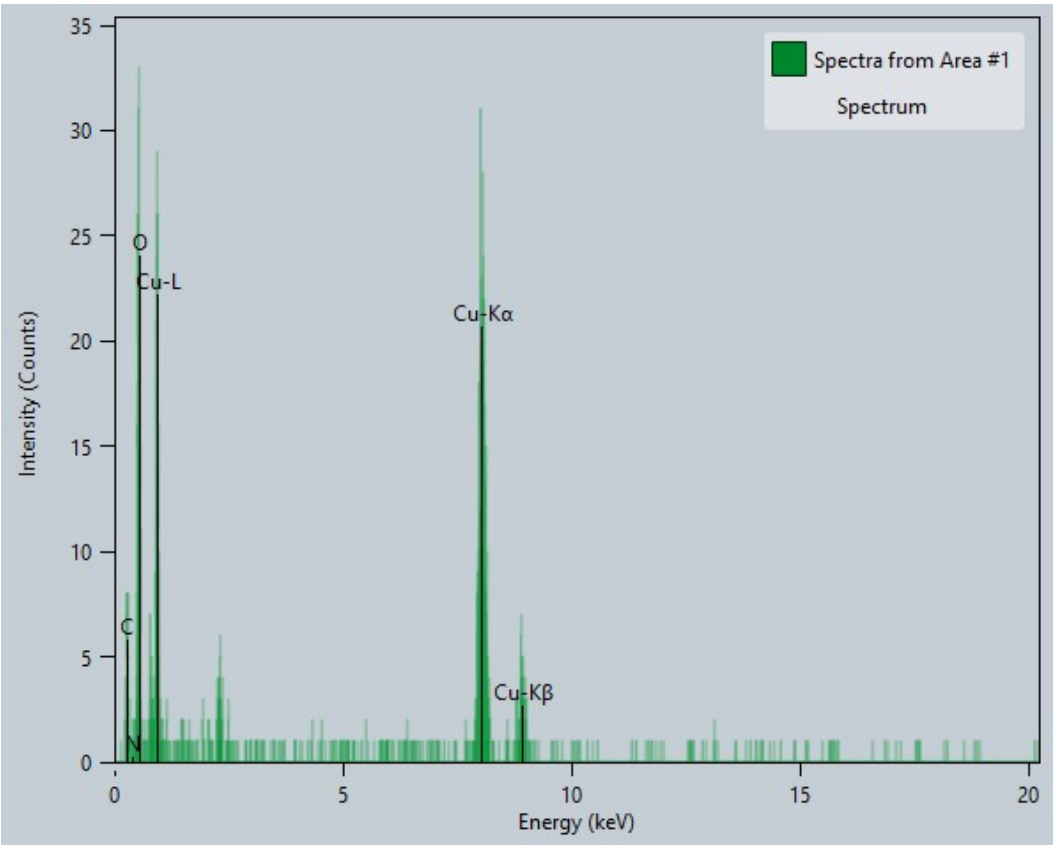

Fig. S3 EDS spectra of PEB-COP-Cu.

Section 7. UV-visible spectra and working curve of PEB-COP-Cu.

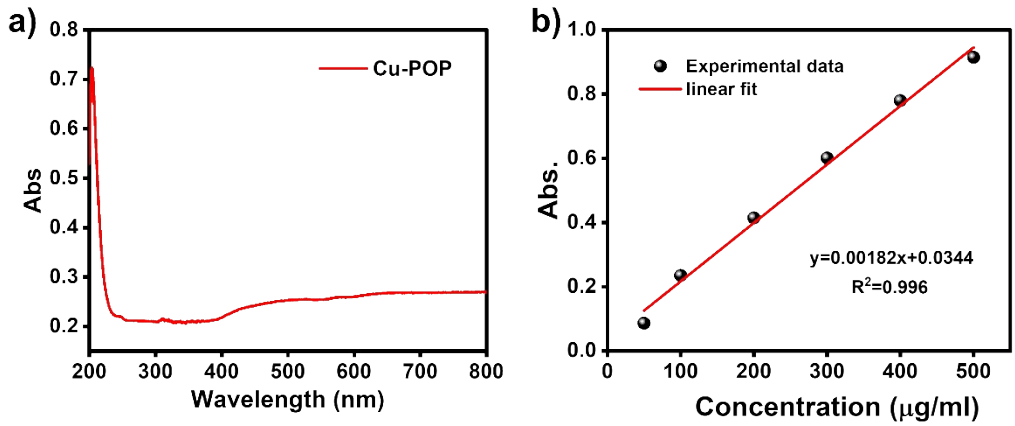

Fig. S4 a) UV-visible spectra of PEB-COP-Cu; b) Absorbance versus concentration working curve of PEB-COP-Cu.

Section 8. Light and water stability of PEB-COP-Cu.

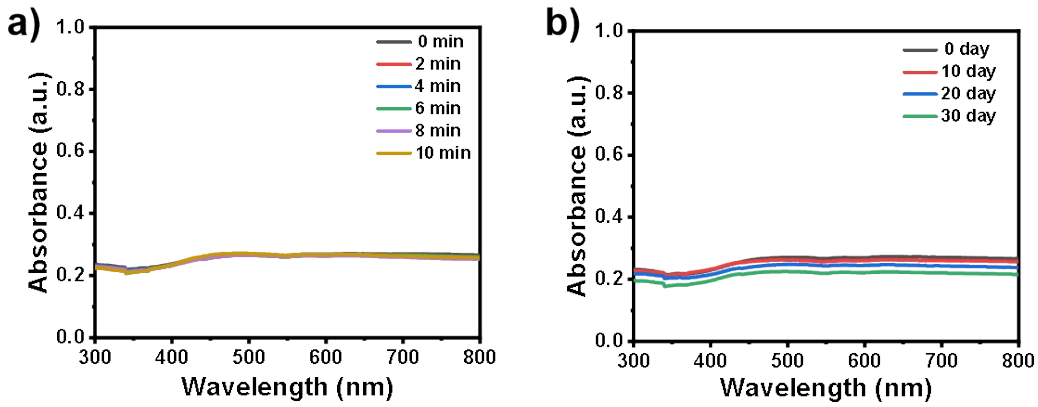

Fig.S5 a) Changes in UV absorption of PEB-COP-Cu after different times (0, 2, 4, 6, 8, 10 min) of 638 nm laser irradiation; b) Changes in UV absorption of PEB-COP-Cu after storage in water for different periods of time (0, 10, 20, 30 day).

Section 9. Effect of temperature on the POD and OXD enzyme activities of PEG-COP-Cu

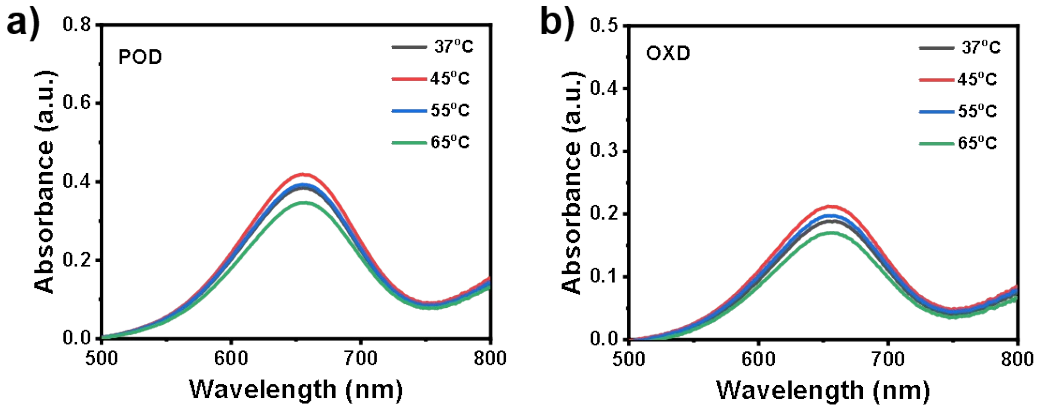

Fig. S6 a)The effect of different temperatures on POD enzyme activity; b)The effect of different temperatures on OXD enzyme activity

Section 10. Photothermal antibacterial effects of PEB-COP-Cu at different concentrations.

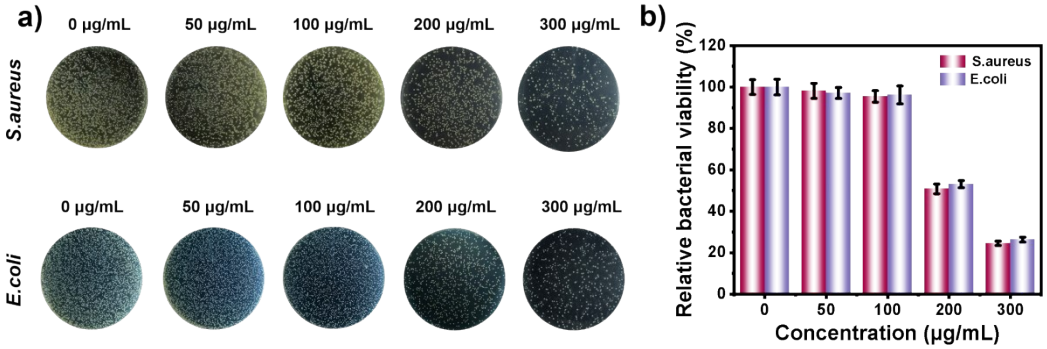

Fig. S7 a) Bacterial images of photothermal treatment of S.aureus and E. coli with PEG-COP-Cu; b) Bacterial survival rate after photothermal treatment of S. aureus and E. coli.

Section 11. Biocompatibility testing of PEB-COP-Cu.

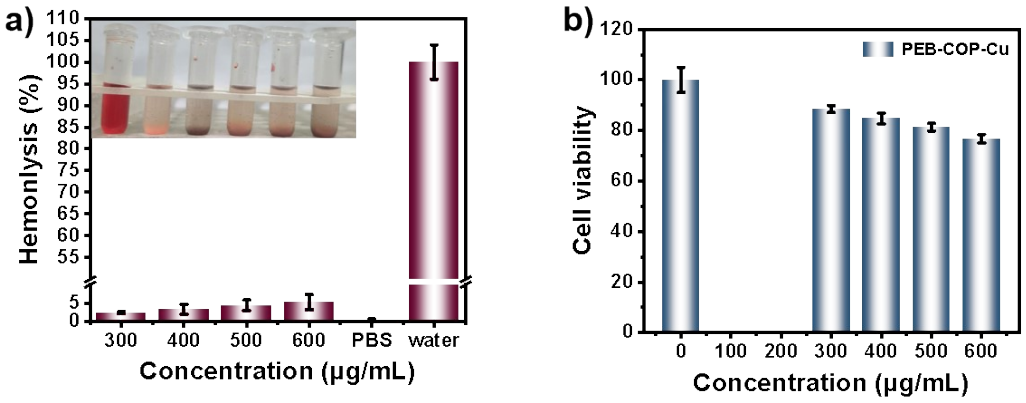

Fig. S8 a) Effect of the concentration of PEB-COP-Cu on the hemolysis rate; b) Effect of the concentration of PEB-COP-Cu on the viability of 3T3 cells.

Section 12. Blood tests in PEB-COP-Cu treated mice.

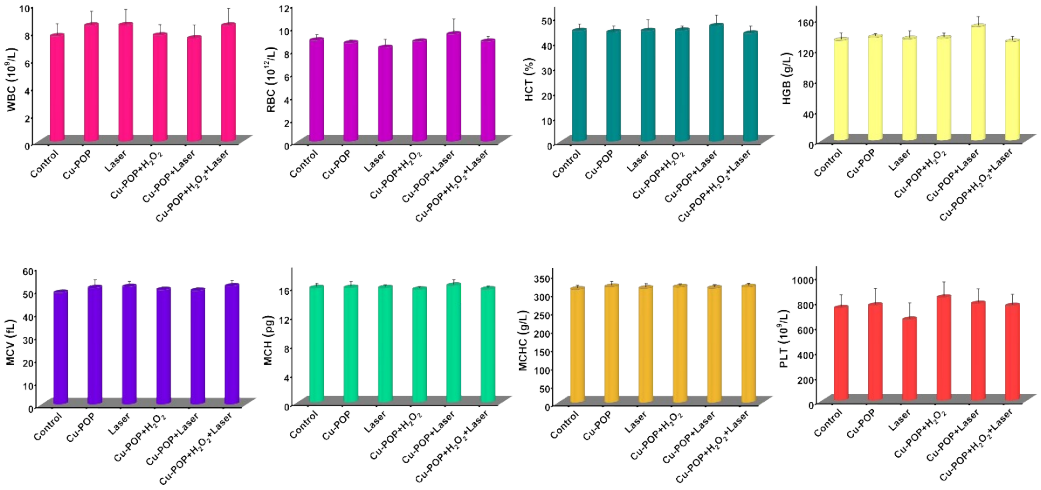

Fig. S9 Blood tests in PEB-COP-Cu treated mice.

Section 13. Supporting Table

Table S1. PCE of recently reported POP-based photothermal agent.

Sample	Power density (W/cm^2)	Laser wavelength (nm)	PCE (%)	Reference
ATP@Au-CuNPs	2	808	59.3	[2]
BiOI@Bi_2S_3 /MXene	1.5	808	57.8	[3]
AuPtNDs	1	808	50.3	[4]
PDA-NH2@Ag	1	808	49.6	[5]
PANi/TiO_2 /$Ti_3C_2T_x$	1.5	808	43.3	[6]
PEB-COP-Cu	1.5	638	42.6	This work
BODIPY-Mo_2C	1.5	808	42.6	[7]
Au-Cu JNSs	1	1064	42.1	[8]
GaHA@PDA	2	808	41.2	[9]
GelMA/CeO_2/PDA	1	808	40	[10]
Cu_xO@PDA (CP)	1.5	808	39.81	[11]
Mo_{154} /TK-14	1.4	808	38.6	[12]
CuS nanoflowers	1	1064	37.60	[13]
MSN@Au-Fc	2	808	35.9	[14]
PDA NPs	1.6	808	32	[15]
ZIF-8/Ag/PDA	1	808	31	[16]
CuSe / PVDF	2	1064	30.8	[17]
ZIF-8-TA/PBQDs	1	808	27.92	[18]
Fe-N-C Sazyme	1.5	808	23.3	[19]
PLLA/CeO2@PDA/Ag	1.5	808	21	[20]

Section 14. Supporting References

[1] Y. Liu, Y. Wang, H. Li, X. Guan, L. Zhu, M. Xue, Y. Yan, V. Valtchev, S. Qiu,Q. Fang, Ambient aqueous-phase synthesis of covalent organic frameworks for degradation of organic pollutants. *Chemical Science.10 (2019) 10815-10820.*

[2] Q. Song, Y. Liu, P. Zhang, W. Feng, S. Shi, N. Zhou, X. Chu,J. Shen, Au–Cu Bimetallic Nanostructures for Photothermal Antibacterial and Wound Healing Promotion. *ACS Applied Nano Materials.5 (2022) 8621-8630.*

[3] H. Feng, W. Wang, T. Wang, Y. Pu, C. Ma,S. Chen, Interfacial regulation of BiOI@Bi2S3/MXene heterostructures for enhanced photothermal and photodynamic therapy in antibacterial applications. *Acta Biomaterialia.171 (2023) 506-518.*

[4] S. Zhang, Q. Lu, F. Wang, Z. Xiao, L. He, D. He,L. Deng, Gold–Platinum Nanodots with High-Peroxidase-like Activity and Photothermal Conversion Efficiency for Antibacterial Therapy. *ACS Applied Materials & Interfaces.13 (2021) 37535-37544.*

[5] X. Li, H. Shang, Y. Xiong, Y. Luan, D. Wang,X. Du, Silver/jellyfish-like mesoporous polydopamine nanomotor with concentration-dependent synergistic antibacterial activity. *Chemical Engineering Journal.505 (2025) 159367.*

[6] C. Jin, D. Sun, Z. Sun, S. Rao, Z. Wu, C. Cheng, L. Liu, Q. Liu,J. Yang, Interfacial engineering of Ni-phytate and Ti3C2Tx MXene-sensitized TiO2 toward enhanced sterilization efficacy under 808 nm NIR light irradiation. *Applied Catalysis B: Environmental.330 (2023) 122613.*

[7] Q. Lv, Y. Zhou, L. Wang, S. Zhu, H. Lu, W. Yang,C. Wei, Mo2C nanosheets decorated with boron dipyrromethene enabling photothermal and photodynamic attributes for highly efficient antibacterials. *Applied Surface Science.652 (2024) 159216.*

[8] Q. Yang, H. Kong, L. Tang, Y. Ma, F. Liu, M. Liu, Y. Wang, P. Zhang,Y. Zheng, Au–Cu Janus Nanostructures as NIR-II Photothermal Antibacterial Agents. *ACS Applied Nano Materials.7 (2024) 20783-20792.*

[9] C. Wang, H. Kang, Y. Liu, R. Yin, X. Yuan, A. Cai, Z. Yue, C. Zhang,C. Qian, Synergistic Effect of Polydopamine and Gallium Ion Doping on Photothermal and Antibacterial Properties of Hydroxyapatite. *Journal of Inorganic and Organometallic Polymers and Materials.35 (2025) 625-640.*

[10] Y. Xue, F. Yang, Y. He, F. Wang, D. Xia,Y. Liu, Multifunctional Hydrogel with Photothermal ROS Scavenging and Antibacterial Activity Accelerates Diabetic Wound Healing. *Advanced Healthcare Materials.n/a 2402236.*

[11] L. Luo, W. Zhang, W. Su, J. Zhuo, L. Zhang, X. Xie, W. Zhang,J. Wang, A Robust Photothermal-Mediated Nanozyme Engineering with Efficient Synergistic Antibacterial Therapy for Wound Healing. *ACS Materials Letters.6 (2024) 2487-2496.*

[12] Y. Wang, G. Chen, R. Liu, X. Fang, F. Li, L. Wu,Y. Wu, Synergistically enhanced photothermal transition of a polyoxometalate/peptide assembly improved the antibiofilm and antibacterial activities. *Soft Matter.18 (2022) 2951-2958.*

[13] Y. Jiao, S. Wu, Y. Wang, F. Liu, M. Liu, Y. Wang, P. Zhang, Y. Wang,Y. Zheng, Fatty Amine-Mediated Synthesis of Hierarchical Copper Sulfide Nanoflowers for Efficient NIR-II Photothermal Conversion and Antibacterial Performance. *Langmuir.40 (2024) 604-613.*

[14] Y. Bai, J. Wu, K. Liu, X. Wang, Q. Shang,H. Zhang, Integrated supramolecular nanovalves for photothermal augmented chemodynamic therapy through strengthened amplification of oxidative stress. *Journal of Colloid and Interface Science.637 (2023) 399-407.*

[15] Y. Zhang, K. Zhang, H. Yang, Y. Hao, J. Zhang, W. Zhao, S. Zhang, S. Ma,C. Mao, Highly

Penetrable Drug-Loaded Nanomotors for Photothermal-Enhanced Ferroptosis Treatment of Tumor. *ACS Applied Materials & Interfaces.15 (2023) 14099-14110.*

[16] J. Lin, Y. Li, L. Ge, Y. Zhang, S. Yuan, M. Wang, D. Xu,J. Tu, Photothermal enhanced ion release of ZIF-8/Ag/PDA for boosted antimicrobial performance. *Inorganic Chemistry Communications.174 (2025) 114001.*

[17] X.-M. Wang, L. Huang, Y.-J. Wang, L. Xuan, W.-W. Li,L.-J. Tian, Highly efficient near-infrared photothermal antibacterial membrane with incorporated biogenic CuSe nanoparticles. *Chemical Engineering Journal.405 (2021) 126711.*

[18] J. Wang, S. Zhou, F. Lu, S. Wang,Q. Deng, Polyphenols functionalized MOF encapsulated BPQDs for synergistic photothermal/photodynamic antibacterial properties and multifunctional food preservation. *Food Chemistry.451 (2024) 139451.*

[19] Y. Feng, J. Qin, Y. Zhou, Q. Yue,J. Wei, Spherical mesoporous Fe-N-C single-atom nanozyme for photothermal and catalytic synergistic antibacterial therapy. *Journal of Colloid and Interface Science.606 (2022) 826-836.*

[20] Y. Ma, Y. Zhang, H. Osman, D. Zhang, T. Zhou, Y. Zhang,Y. Wang, In Situ Photoactivated Antibacterial and Antioxidant Composite Materials to Promote Bone Repair. *Macromolecular Bioscience.24 (2024) 2400079.*